

Rotational diffusion measurements of suspended colloidal particles using two-dimensional exchange nuclear magnetic resonance

G. A. Barrall, K. Schmidt-Rohr,^{a)} Y. K. Lee,^{b)} K. Landfester,^{c)} H. Zimmermann,^{d)}
G. C. Chingas,^{e)} and A. Pines

*Materials Sciences Division, Lawrence Berkeley Laboratory, Berkeley, California 94720
and Department of Chemistry, University of California, Berkeley, California 94720*

(Received 5 July 1995; accepted 25 September 1995)

We present here an experimental and theoretical study of the application of two-dimensional exchange nuclear magnetic resonance spectroscopy (NMR) to the investigation of the rotational diffusion of colloidal particles. The theoretical discussion includes the nature of the NMR frequency time-correlation function where the NMR interaction is represented by the chemical shift anisotropy (CSA). Time-correlation functions for the isotropic rotational diffusion of a suspension of colloidal particles containing single and multiple sites are derived in addition to time-correlation functions for the rotational diffusion of a suspension of symmetric top particles containing an isotropic distribution of a single CSA interaction. Simulations of two-dimensional exchange spectra for particles undergoing isotropic rotational diffusion are presented. We performed two-dimensional exchange NMR experiments on a colloidal suspension of spherical poly(methyl methacrylate) (PMMA) particles which were synthesized with a 20% enrichment in ^{13}C at the carbonyl site. Rotational diffusion time-correlation functions determined from the experimental exchange spectra are consistent with the composition of the colloidal suspension. Detailed explanations of the syntheses of the enriched methyl ^{13}C -(carbonyl)-methacrylate monomer and the small quantities of 20% enriched ^{13}C -(carbonyl)-poly(methyl methacrylate) microspheres used for this study are presented. © 1996 American Institute of Physics. [S0021-9606(96)00301-5]

I. INTRODUCTION

In this work, we present a new application of two-dimensional exchange nuclear magnetic resonance spectroscopy (NMR) to study the classical reorientational dynamics of macroscopic (i.e., much larger than molecular size) particles in suspension. Two-dimensional exchange NMR has been used previously to study the reorientational dynamics of large molecules in the solid or near solid state for time scales from milliseconds to seconds.¹⁻³ When reorientation on the molecular scale is negligible, the technique may be applied equally well to probe the reorientation of macroscopic rigid bodies. Here we demonstrate the application of the technique to the study of the rotational diffusion of latex spheres in suspension.

To date, dynamic light scattering (DLS) and depolarized dynamic light scattering (DDLS) have been the most widely used techniques to study the dynamics of colloidal suspensions, and have provided a wealth of information about the translational and rotational diffusion of suspended particles and macromolecules.⁴⁻⁶ These techniques, however, are lim-

ited by a number of drawbacks. The solution must be free of any impurities which may cause unwanted scattering, solutions which are opaque to the light source are not accessible, and in order to observe rotational diffusion, the scatterer must be optically anisotropic^{4,5} or have some physical anisotropy. Further complications arise in the study of dense systems which produce large amounts of multiple scattering.

Two-dimensional exchange NMR offers a number of advantages to DLS. Chemical selectivity allows the measurement of dynamics in the presence of impurities, the sample need not be optically clear, and solutions of very high concentration may be easily studied. In fact, concentrated solutions are preferred due to the low sensitivity of the NMR technique. Here, we will introduce the techniques used for the study of the rotational diffusion of latex particles in suspension and the methods used to simulate the experiments and extract information about the isotropic rotational diffusion constant.

The technique relies on the orientation dependence of NMR frequencies in the solid state. This study confines itself to the use of the ^{13}C chemical shift anisotropy (CSA) as a probe. One may alternatively use any similar orientationally dependent interaction, such as the quadrupolar interaction of ^2H .⁷ ^{13}C was used in this study, as we found it possible to produce monodisperse latex microspheres enriched in this isotope.

II. THEORY

A. Two-dimensional exchange NMR of ^{13}C

A spin-1/2 nucleus possessing a chemical shift anisotropy has an orientation dependent frequency given by⁸

^{a)}Present address: Department of Polymer Science and Engineering, University of Massachusetts, Amherst, Massachusetts 01003.

^{b)}Graduate Group in Biophysics, University of California, Berkeley, California 94720.

^{c)}Max Planck Institut für Polymerforschung, Ackermannweg 10, 55128 Mainz, Germany.

^{d)}Max Planck Institut für Medizinische Forschung, Jahnstrasse 29, D-69120 Heidelberg, Germany.

^{e)}Present address: Center for Functional Imaging, Life Sciences Division, Lawrence Berkeley Laboratory, 1 Cyclotron Road, Berkeley, California 94720.

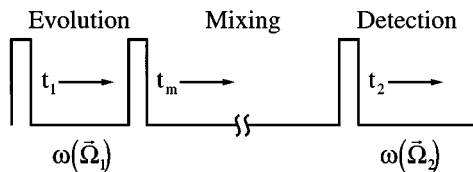


FIG. 1. Basic layout of a two-dimensional NMR exchange experiment. NMR magnetization produced by the first pulse evolves with a frequency related to the initial orientation of the interaction. Evolution of the magnetization ceases during the mixing period to resume during the detection period. During the detection period the magnetization evolves at frequencies determined by the final orientation of the interaction. The mixing period, during which reorientation occurs, is assumed to be much longer than both the evolution and detection periods.

$$\omega(\mathbf{\Omega}) = \sigma + \delta \left\{ \frac{3 \cos^2(\beta) - 1}{2} - \frac{\eta}{2} [\sin^2(\beta) \cos(2\alpha)] \right\}, \quad (1)$$

where σ is the isotropic chemical shift, δ is the chemical shift anisotropy, and η is the asymmetry parameter. The notation used here is slightly different from that of Haeberlen⁸ in that we have not included a multiplicative constant ω_0 on the right-hand side of Eq. (1). As we will only be working at one static field strength, this term will not change, so we have decided to absorb it into the values for σ and δ . We make the standard assumptions for this type of experiment concerning the nature of the NMR interaction and the evolution of the nuclear spin magnetization, namely, the NMR interaction will consist only of the chemical shift anisotropy of a spin-half nucleus such as ¹³C, complete dipolar decoupling of ¹³C and ¹H nuclei is achieved during evolution and detection, all CSA parameters are constant in time, all rf pulses are “hard,” i.e., they will be assumed to be delta functions, there is no spin diffusion, and spin-lattice relaxation is independent of the orientation of the CSA tensor.

The Euler angle triplet $\mathbf{\Omega} = (\alpha, \beta, \gamma)$ is the orientation of the CSA principal axis system (PAS) relative to the static magnetic field \mathbf{B}_0 or laboratory system (LS). Strictly speaking, it is only necessary to take into account two angles for the CSA frequency, but we will be using the vector $\mathbf{\Omega}$ to denote orientation in three dimensional space in later sections. In defining orientation using the Euler angles, we will use the convention of Rose.⁹

Since the latex particles contain randomly oriented polymer chains, the spectrum of each particle is a powder pattern, and the time domain signal, $F(t)$, acquired in a simple one dimensional experiment for a single latex sphere or a collection of spheres is given by

$$F(t) = \frac{1}{8\pi^2} \int d\mathbf{\Omega} \exp[i\omega(\mathbf{\Omega})t], \quad (2)$$

where the differential $d\mathbf{\Omega} = \sin(\beta) d\alpha d\beta d\gamma$, and for an isotropic sample, the integration proceeds from 0 to 2π for α and γ , and from 0 to π for β .

The form of the two-dimensional NMR experiment¹⁰ is given in Fig. 1. After the initial excitation of the ¹³C magne-

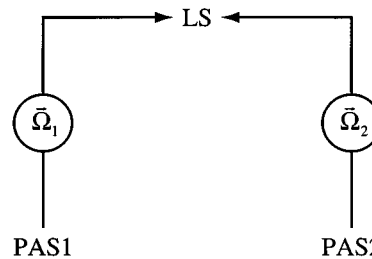


FIG. 2. Order of rotations relating the principal axis systems (PAS1 and PAS2) of the CSA tensor during mixing and detection to the laboratory system (LS).

tization, each spin evolves for a time t_1 at the frequency dictated by its initial orientation,

$$\omega(\mathbf{\Omega}_1) = \sigma + \delta \left\{ \frac{3 \cos^2(\beta_1) - 1}{2} - \frac{\eta}{2} [\sin^2(\beta_1) \cos(2\alpha_1)] \right\}. \quad (3)$$

The initial orientation $\mathbf{\Omega}_1$ will be referred as PAS1, Fig. 2. After the evolution period, a second pulse stores one component of the magnetization parallel to \mathbf{B}_0 for a mixing time t_m , during which physical reorientation may occur, thus changing the relative orientation of the PAS to the LS. The third pulse returns the spin magnetization to the transverse plane for detection. During detection, each spin will evolve at a frequency determined by its new orientation $\mathbf{\Omega}_2$ referred to as PAS2,

$$\omega(\mathbf{\Omega}_2) = \sigma + \delta \left\{ \frac{3 \cos^2(\beta_2) - 1}{2} - \frac{\eta}{2} [\sin^2(\beta_2) \cos(2\alpha_2)] \right\}. \quad (4)$$

The resulting two-dimensional time domain signal is an ensemble average of the spin isochromats over all possible initial and final orientations weighted by the joint probability density for the reorientation from PAS1 to PAS2,

$$\begin{aligned} F(t_1, t_2) &= \langle \exp[i\omega(\mathbf{\Omega}_1)t_1] \exp[i\omega(\mathbf{\Omega}_2)t_2] \rangle \\ &= \int d\mathbf{\Omega}_1 \int d\mathbf{\Omega}_2 W(\mathbf{\Omega}_1, 0) P(\mathbf{\Omega}_2, t_m | \mathbf{\Omega}_1, 0) \\ &\quad \times \exp[i\omega(\mathbf{\Omega}_1)t_1] \exp[i\omega(\mathbf{\Omega}_2)t_2], \end{aligned} \quad (5)$$

where $P(\mathbf{\Omega}_2, t_m | \mathbf{\Omega}_1, 0)$ is the conditional probability density that a CSA tensor with an initial orientation $\mathbf{\Omega}_1$ will reorient to a final PAS at $\mathbf{\Omega}_2$ in a time t_m . In this case, $W(\mathbf{\Omega}_1, 0)$ represents the probability that the CSA tensor is oriented at $\mathbf{\Omega}_1$ at time $t=0$, and as we are dealing with isotropic samples, this term is a constant, $1/8\pi^2$. Two-dimensional Fourier transformation of the time domain signal yields the frequency spectrum

$$S(\omega_1, \omega_2; t_m) = \int d\Omega_1 \int d\Omega_2 \delta[\omega(\Omega_1) - \omega_1] \delta[\omega(\Omega_2) - \omega_2] W(\Omega_1, 0) P(\Omega_2, t_m | \Omega_1, 0). \quad (6)$$

In this case, δ refers to the Dirac delta function not to the anisotropy parameter. Equation (6) will provide the means to extract information about reorientational dynamics directly from the frequency domain NMR signal.

Depending upon the nature of the reorientational process, one will need to consider different functional forms for the joint reorientational probability density. In this study, we assume that the particles undergo isotropic rotational diffusion for which the basic theory is presented in the next section. We also desire some means of extracting quantitative information about the isotropic rotational diffusion constant, from which one may determine the size of the latex microspheres in solution. In analogy with DLS where such information is often extracted from the time-correlation function of the scattered light, we will develop equations describing the time-correlation function of the NMR frequency and also a means of extracting the NMR frequency time-correlation function directly from the two-dimensional exchange spectrum.

B. Isotropic rotational diffusion

The equation of motion for an isolated rigid particle undergoing rotational Brownian diffusion is given by

$$\frac{\partial W(\Omega, t)}{\partial t} + (\mathbf{L} \cdot \mathbf{D} \cdot \mathbf{L}) W(\Omega, t) = 0, \quad (7)$$

where $W(\Omega, t)$ is the probability density for the particle to have orientation Ω at time t , \mathbf{L} is the infinitesimal rotation operator, and \mathbf{D} is the rotational diffusion tensor. The formal solution to Eq. (7) is¹¹

$$W(\Omega, t) = \int d\Omega_1 W(\Omega_1, 0) P(\Omega, t | \Omega_1, 0), \quad (8)$$

where $W(\Omega_1, 0)$ is the probability that the particle has an initial orientation Ω_1 , and $P(\Omega, t | \Omega_1, 0)$ is the conditional probability that if the particle was initially at Ω_1 , then it will have the orientation Ω at time t . For the case of isotropic rotational diffusion, it has been shown that^{11,12}

$$\begin{aligned} W(\Omega_1, 0) P(\Omega, t | \Omega_1, 0) &= \frac{1}{8\pi^2} \sum_{l=1}^{\infty} \left\{ \frac{2l+1}{8\pi^2} \exp[-l(l+1)D^r t] \right. \\ &\quad \left. \times \sum_{m=-l}^l \sum_{n=-l}^l \mathcal{D}_{mn}^l(\Omega_1)^* \mathcal{D}_{mn}^l(\Omega) \right\}. \end{aligned} \quad (9)$$

The terms \mathcal{D}_{mn}^l are Wigner rotation matrix elements, and D^r is the isotropic rotational diffusion constant in Hz.

At infinite dilution, D^r has a particularly simple form,¹³

$$D_0^r = \frac{k_B T}{8\pi\nu a^3}, \quad (10)$$

where k_B is the Boltzmann constant, T is the temperature, ν is the viscosity of the suspending fluid, and a is the hydrodynamic radius of the colloidal particle. For finite dilution reorientation appears diffusive for short observation times with the diffusion coefficient dependent upon the relative volume fraction, ϕ , of the colloidal particles,¹⁴

$$D^r = D_0^r (1 - C^r \phi). \quad (11)$$

The coefficient C^r is dependent upon the nature of the interaction between the particles and the suspending fluid and has the value 0.63 for the case of hard spheres with no-slip hydrodynamic boundary conditions.¹⁴ In the following sections, we will use the corrected form of the rotational diffusion coefficient given in Eq. (11) and $C^r = 0.63$.

C. Time-correlation functions

The diffusion statistics can be fully described by the normalized orientational time-correlation functions given by¹⁵

$$C_{l'm'n',lmn}(t) = \frac{\langle \mathcal{D}_{m'n'}^{l'}[\Omega_1(0)] \mathcal{D}_{mn}^l[\Omega_2(t)]^* \rangle}{\langle |\mathcal{D}_{m'n'}^{l'}[\Omega_1(0)]|^2 \rangle}. \quad (12)$$

The $\langle \rangle$'s refer to the integration over all possible initial and final orientations weighted by the joint reorientational probability density, $W(\Omega_1, 0) P(\Omega_2, t | \Omega_1, 0)$. The orientational time-correlation functions play a central role in DLS, and as we will show in the next section, they also play an important role in interpreting two-dimensional exchange spectra. From the orthogonality of the Wigner rotation matrices,⁹

$$\int d\Omega \mathcal{D}_{m'n'}^{l'}(\Omega) \mathcal{D}_{mn}^l(\Omega)^* = \frac{8\pi^2}{2l+1} \delta_{l'l} \delta_{m'm} \delta_{n'n}, \quad (13)$$

and using the joint reorientational probability density in Eq. (9), we find

$$\begin{aligned} \langle \mathcal{D}_{m'n'}^{l'}(\Omega_1) \mathcal{D}_{mn}^l(\Omega_2)^* \rangle_{ird} &= \frac{1}{2l+1} \exp[-l(l+1)D^r t] \delta_{l'l} \delta_{m'm} \delta_{n'n}, \end{aligned} \quad (14)$$

where the subscript *ird* signifies that the reorientational process is isotropic rotational diffusion. In the two-dimensional exchange NMR experiment we will be particularly interested in the time-correlation functions with $l=2$,

$$C_{2,m}^{ird}(t) = \frac{\langle \mathcal{D}_{m0}^2(\Omega_1) \mathcal{D}_{m0}^2(\Omega_2)^* \rangle_{ird}}{\langle |\mathcal{D}_{m0}^2(\Omega_1)|^2 \rangle} = \exp(-6D^r t), \quad (15)$$

where

$$\langle |\mathcal{D}_{m0}^2(\Omega_1)|^2 \rangle = \frac{1}{5}.$$

For time-correlation functions of this type, it is convenient to define a correlation time given by

$$\tau_c = \frac{1}{6D^r}. \quad (16)$$

Theoretical evidence predicts nonexponential behavior for $C_{2,m}(t)$ in colloidal suspensions of finite dilution, but it is unlikely this behavior will be seen for volume fractions below 0.1.¹⁶

D. Time-correlation functions in two-dimensional exchange NMR for the rotational diffusion of a spherical top

Our objective in this section is to find a method to extract the time-correlation function and, therefore, information about the rotational diffusion constant for a spherically symmetric diffuser directly from the two-dimensional exchange spectrum.

The frequency of the CSA interaction with $\sigma=0$ and $\delta=1$ in terms of the Wigner rotation matrices⁸ is

$$\omega(\mathbf{\Omega}) = \mathcal{D}_{00}^2(\mathbf{\Omega}) + \frac{\eta}{\sqrt{6}} [\mathcal{D}_{20}^2(\mathbf{\Omega}) + \mathcal{D}_{-20}^2(\mathbf{\Omega})]. \quad (17)$$

Although it is not necessary to set the isotropic chemical shift to zero, we have decided to do so in the actual calculations of the NMR frequency time-correlation function. The case where σ is not set to zero will be discussed later in this section where we will investigate the consequences of overlapping CSA powder patterns arising from chemically distinct sites. Because $\omega(\mathbf{\Omega})$ is real, we may express the NMR frequency time-correlation function in terms of the time-correlation functions discussed in the previous section,

$$\begin{aligned} & \langle \omega(\mathbf{\Omega}_1) \omega(\mathbf{\Omega}_2) \rangle \\ &= \langle \omega(\mathbf{\Omega}_1) \omega(\mathbf{\Omega}_2)^* \rangle \\ &= \langle \mathcal{D}_{00}^2(\mathbf{\Omega}_1) \mathcal{D}_{00}^2(\mathbf{\Omega}_2)^* \rangle + \sqrt{\frac{2}{3}} \eta \langle \mathcal{D}_{00}^2(\mathbf{\Omega}_1) [\mathcal{D}_{20}^2(\mathbf{\Omega}_2)^* \\ &+ \mathcal{D}_{-20}^2(\mathbf{\Omega}_2)^*] \rangle + \frac{\eta^2}{6} \langle [\mathcal{D}_{20}^2(\mathbf{\Omega}_1) + \mathcal{D}_{-20}^2(\mathbf{\Omega}_1)] \\ &\times [\mathcal{D}_{20}^2(\mathbf{\Omega}_2)^* + \mathcal{D}_{-20}^2(\mathbf{\Omega}_2)^*] \rangle. \end{aligned} \quad (18)$$

Using Eq. (9) and the relation derived in Eq. (14), we arrive at the desired expression for the normalized isotropic rotational diffusion time-correlation function of the CSA frequency, which we shall denote $C_2^{cs}(t_m)$,

$$C_2^{cs}(t_m) = \frac{\langle \omega(\mathbf{\Omega}_1) \omega(\mathbf{\Omega}_2)^* \rangle_{ird}}{\langle |\omega(\mathbf{\Omega}_1)|^2 \rangle} = \exp(-6D^r t_m), \quad (19)$$

where

$$\langle |\omega(\mathbf{\Omega}_1)|^2 \rangle = \frac{1}{5} \left(1 + \frac{\eta^2}{3} \right).$$

This is identical to the time-correlation function found in Eq. (15) except the normalization is given by $(1 + \eta^2/3)/5$ as opposed to $1/5$. In the case of an axially symmetric CSA interaction ($\eta=0$), the normalization factors in Eqs. (15) and (19) are identical.

In deriving Eq. (19), we did not need to consider the relative orientation of the CSA interaction within the diffusing particles. Due to the symmetry of the motion, one may in

fact view the situation as merely the isotropic rotational diffusion of a collection of CSA tensors. We shall see in the next section that this viewpoint is not correct when the diffuser is nonspherical.

There exists one more crucial step to developing a method to determine C_2^{cs} directly from the experimentally obtained two-dimensional exchange spectrum. Using a modification of the expression for the frequency domain NMR signal given in Eq. (6) where we have replaced $\omega(\mathbf{\Omega}_2)$ by its complex conjugate, one can easily show that

$$\begin{aligned} & \int d\omega_1 \int d\omega_2 S(\omega_1, \omega_2; t_m) \omega_1 \omega_2 \\ &= \int d\mathbf{\Omega}_1 \int d\mathbf{\Omega}_2 W(\mathbf{\Omega}_1, 0) \\ &\quad \times P(\mathbf{\Omega}_2, t_m | \mathbf{\Omega}_1, 0) \omega(\mathbf{\Omega}_1) \omega(\mathbf{\Omega}_2)^*, \end{aligned} \quad (20)$$

where we have assumed that the exchange spectrum is normalized,

$$\int d\omega_1 \int d\omega_2 S(\omega_1, \omega_2; t_m) = 1. \quad (21)$$

From Eq. (19) and Eq. (20),

$$C_2^{cs}(t_m) = \frac{\int d\omega_1 \int d\omega_2 S(\omega_1, \omega_2; t_m) \omega_1 \omega_2}{\frac{1}{5} \left(1 + \frac{\eta^2}{3} \right)}. \quad (22)$$

This result for the case of $\eta=0$, where $C_2^{cs}(t_m) = C_{2,0}(t_m)$, was previously reported by Schmidt-Rohr and Spiess.^{1,17} In Eqs. (20) and (22), we are assuming that the weighted integral of the spectrum is carried out from $-(1+\eta)/2$ to 1 for both ω_1 and ω_2 , in a frequency space which is scaled such that $\delta=1$ and $\sigma=0$. We do not carry out the integration over a region larger than that determined by the spectrum, since in a real experiment the presence of noise outside of the region of interest may adversely affect the results. In order to do this, of course, it is necessary to know all three CSA parameters.

We now have a relatively direct method of extracting isotropic rotational diffusion information from the two-dimensional exchange NMR experiment. In fact, the exchange experiment is actually simpler to interpret than the DDLS experiment as the light-scattering time-correlation functions also contain an exponential decay arising from translational diffusion.¹⁵

Although we are primarily concerned with measuring time-correlation functions in a system with an isolated chemical shift where it is possible to zero the isotropic frequency by changing the reference frequency, many potentially interesting systems contain multiple sites with overlapping CSA powder patterns. In this case, it is not generally possible to choose a single reference frequency for which all of the isotropic frequencies are zero. We then have a NMR spectrum which consists of a sum over the spectra produced by each site

$$S(\omega_1, \omega_2; t_m) = \sum_{i=1}^{n_{\text{sites}}} C_i S_i(\omega_1, \omega_2; t_m), \quad (23)$$

where n_{sites} is the number of chemically distinct sites being observed, and C_i is the relative population of the i th site. Using Eq. (20) and the fact that integration is distributive,

$$\begin{aligned} & \int d\omega_1 \int d\omega_2 S(\omega_1, \omega_2; t_m) \omega_1 \omega_2 \\ &= \sum_{i=1}^{n_{\text{sites}}} C_i \int d\omega_1 \int d\omega_2 S_i(\omega_1, \omega_2; t_m) \omega_1 \omega_2 \\ &= \sum_{i=1}^{n_{\text{sites}}} C_i \langle \omega_i(\mathbf{\Omega}_1) \omega_i(\mathbf{\Omega}_2)^* \rangle. \end{aligned} \quad (24)$$

We now must compute the time-correlation function for NMR frequencies of the form

$$\omega_i(\mathbf{\Omega}) = \sigma_i + \delta_i \left\{ \mathcal{D}_{00}^2(\mathbf{\Omega}) + \frac{\eta_i}{\sqrt{6}} [\mathcal{D}_{20}^2(\mathbf{\Omega}) + \mathcal{D}_{-20}^2(\mathbf{\Omega})] \right\}, \quad (25)$$

where this time we have included the isotropic chemical shift and the anisotropy. For any of the given sites we find that the isotropic rotational diffusion NMR frequency time-correlation function is

$$\langle \omega_i(\mathbf{\Omega}_1) \omega_i(\mathbf{\Omega}_2)^* \rangle_{\text{ind}} = \sigma_i^2 + \left[\frac{\delta_i^2}{5} \left(1 + \frac{\eta_i^2}{3} \right) \right] \exp(-6D^r t_m). \quad (26)$$

The frequency weighted integral over the NMR spectrum is then

$$\begin{aligned} & \int d\omega_1 \int d\omega_2 S(\omega_1, \omega_2; t_m) \omega_1 \omega_2 \\ &= \exp(-6D^r t_m) \sum_{i=1}^{n_{\text{sites}}} C_i \left[\frac{\delta_i^2}{5} \left(1 + \frac{\eta_i^2}{3} \right) \right] + \sum_{i=1}^{n_{\text{sites}}} C_i \sigma_i^2. \end{aligned} \quad (27)$$

The limits of the integration in this case should be set so that all of the relevant powder patterns are included in the integration region.

Although Eq. (27) is more complicated than the expression for a single CSA interaction with zero isotropic shift, Eq. (19), if one knows all of the relevant CSA parameters, the determination of the rotational diffusion constant is relatively simple. In the event that one does not know the CSA parameters, one may determine the rotational diffusion constant by treating the two terms containing the CSA parameters as variables in a fit of the experimental data.

The treatment presented here will also be useful for a quantitative analysis of ^2H NMR spectra, where the powder patterns of two NMR transitions overlap. Since the powder patterns have the same center of gravity, σ_i can be chosen to be zero. In addition, the magnitude of δ is the same for both patterns. For the quadrupolar interaction of deuterons bonded

to aliphatic carbons, $\eta \approx 0$. Therefore, the frequency-weighted integral over the ^2H NMR 2D spectrum, Eq. (27), simplifies to $(\delta^2/5) \exp(-6D^r t_m)$.

E. Time-correlation functions in two-dimensional exchange NMR for the rotational diffusion of a symmetric top

Although we intend in this study to investigate the rotational diffusion of spherical particles, it is important to understand the form of the correlation function if the particles are not spherical. In fact, the development of this work was prompted by the appearance of multiple correlation times in the experimental data which will be presented later. Consider, for example, a rodlike particle whose reorientation about the axis of symmetry is rapid with respect to the mixing time, but whose reorientation perpendicular to the axis of symmetry is slow. An axially symmetric CSA interaction parallel to the symmetry axis of the rod will show relatively little frequency exchange for the given mixing time. On the other hand, considerable frequency exchange will occur if the CSA tensor is perpendicular to the symmetry axis of the rod. It is therefore necessary to discuss the orientation of the CSA tensor not only in terms of how the particles are moving, but also in terms of the relative orientation of the CSA tensor and the particle.

The diffusion tensor for a symmetric top may be represented by two diffusion constants, D_{\parallel} and D_{\perp} , in the reference frame, PAS_{diff} , which diagonalizes the diffusion tensor. D_{\parallel} describes the diffusion rate about the axis of symmetry, whereas D_{\perp} describes the diffusion rate perpendicular to the symmetry axis as shown in Fig. 3. As with isotropic rotational diffusion, one may obtain an analytical solution of Eq. (7) for a symmetric top. In this case, the joint reorientational probability density for the diffusor is given by^{11,12}

$$\begin{aligned} & W_{\text{diff}}(\mathbf{\Omega}_1, 0) P_{\text{diff}}(\mathbf{\Omega}_2, t | \mathbf{\Omega}_1, 0) \\ &= \frac{1}{8\pi^2} \sum_{l=1}^{\infty} \left\{ \frac{2l+1}{8\pi^2} \exp[-l(l+1)D_{\perp}t] \right. \\ & \quad \left. - m^2(D_{\parallel} - D_{\perp})t \right] \sum_{m=-l}^l \sum_{n=-l}^l \mathcal{D}_{mn}^l(\mathbf{\Omega}_1)^* \mathcal{D}_{mn}^l(\mathbf{\Omega}_2) \Big\}. \end{aligned} \quad (28)$$

Depending upon one's definition of the Euler angles, the m^2 contained in the exponential will either be the first or the second subscript of the Wigner rotation matrix elements. As stated before, we have chosen to adopt the convention used by Rose.⁹

Unlike the case of the spherical top, where the diffusion tensor is diagonal in any PAS, for the symmetric top the diffusion tensor is only diagonal in PAS_{diff} . Therefore, we must first rotate the PAS of the chemical shift interaction during the encode period, PAS_{CS} , into the PAS which diagonalizes the diffusion tensor during the same period, PAS_{diff} . As we observe the CSA frequency in the LS, we

must perform another rotation of $\text{PAS1}_{\text{diff}}$ to LS. We will denote the first rotation from PAS1_{cs} to $\text{PAS1}_{\text{diff}}$ by $\mathbf{\Omega}'$, and the rotation from $\text{PAS1}_{\text{diff}}$ to LS by $\mathbf{\Omega}_1$, the initial orientation of the diffusor. The total rotation from PAS1_{cs} to LS will be denoted $\mathbf{\Omega}_1'$. During the acquisition period we repeat the process substituting 1's for 2's in the previous explanation (see Fig. 4). From Eq. (17), the NMR frequency as a function of $\mathbf{\Omega}'$ and $\mathbf{\Omega}_1$ is given by

$$\omega(\mathbf{\Omega}_1, \mathbf{\Omega}') = \sum_{n'=-2}^2 \mathcal{D}_{n'0}^2(\mathbf{\Omega}_1) \left\{ \mathcal{D}_{0n'}^2(\mathbf{\Omega}') + \frac{\eta}{\sqrt{6}} [\mathcal{D}_{2n'}^2(\mathbf{\Omega}') + \mathcal{D}_{-2n'}^2(\mathbf{\Omega}')] \right\}. \quad (29)$$

Determination of the time-correlation function requires specifying the orientation ensemble average of the CSA tensor in the particles. In general, we must take into account the probability at $t=0$, $W_{\text{cs}}(\mathbf{\Omega}', 0)$, that PAS1_{cs} has orientation $\mathbf{\Omega}'$ with respect to $\text{PAS1}_{\text{diff}}$, and the conditional probability density, $P_{\text{cs}}(\mathbf{\Omega}', t_m | \mathbf{\Omega}', 0)$, that PAS2_{cs} is then at the same relative orientation at time t_m . For the case of an isotropic distribution of CSA tensors rigidly embedded in the particles,

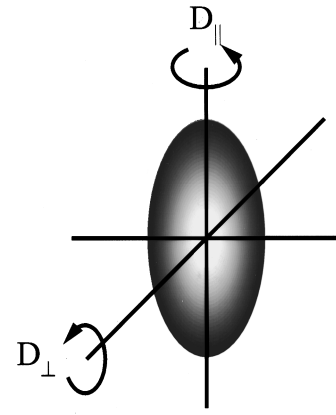


FIG. 3. Relation between the two rotational diffusion coefficients of a symmetric top and the geometry of a prolate ellipsoid. The diffusion coefficient D_{\parallel} refers to diffusion about the axis of symmetry, whereas D_{\perp} refers to diffusion perpendicular to the axis of symmetry.

$$W_{\text{cs}}(\mathbf{\Omega}', 0) = \frac{1}{8\pi^2},$$

$$P_{\text{cs}}(\mathbf{\Omega}', t_m | \mathbf{\Omega}', 0) = 1. \quad (30)$$

Combining Eqs. (28), (29), (30) we arrive at

$$\begin{aligned} \langle \omega(\mathbf{\Omega}_1, \mathbf{\Omega}') \omega(\mathbf{\Omega}_2, \mathbf{\Omega}')^* \rangle &= \left(\frac{1}{8\pi^2} \right)^2 \int d\mathbf{\Omega}_1 \int d\mathbf{\Omega}_2 \int d\mathbf{\Omega}' \sum_{n'=-2}^2 \mathcal{D}_{n'0}^2(\mathbf{\Omega}_1) \left\{ \mathcal{D}_{0n'}^2(\mathbf{\Omega}') + \frac{\eta}{\sqrt{6}} [\mathcal{D}_{2n'}^2(\mathbf{\Omega}') + \mathcal{D}_{-2n'}^2(\mathbf{\Omega}')] \right\} \\ &\times \sum_{n''=-2}^2 \mathcal{D}_{n''0}^2(\mathbf{\Omega}_2)^* \left\{ \mathcal{D}_{0n''}^2(\mathbf{\Omega}')^* + \frac{\eta}{\sqrt{6}} [\mathcal{D}_{2n''}^2(\mathbf{\Omega}')^* + \mathcal{D}_{-2n''}^2(\mathbf{\Omega}')^*] \right\} \\ &\times \sum_{l=0}^{\infty} \sum_{m,n=-l}^l \mathcal{D}_{mn}^l(\mathbf{\Omega}_1)^* \mathcal{D}_{mn}^l(\mathbf{\Omega}_2) \exp[-l(l+1)D_{\perp}t - m^2(D_{\parallel} - D_{\perp})t]. \end{aligned} \quad (31)$$

After carrying out the integrations we obtain

$$\begin{aligned} \langle \omega(\mathbf{\Omega}_1, \mathbf{\Omega}') \omega(\mathbf{\Omega}_2, \mathbf{\Omega}')^* \rangle &= \frac{1}{5} \left(\frac{1}{5} + \frac{\eta^2}{15} \right) \{ 2 \exp[-6D_{\perp}t - 4(D_{\parallel} - D_{\perp})t] \\ &+ 2 \exp[-6D_{\perp}t - (D_{\parallel} - D_{\perp})t] + \exp[-6D_{\perp}t] \}. \end{aligned} \quad (32)$$

One obtains a similar triexponential expression for the depolarized light scattering time-correlation function in DDLs.¹⁵

This result can be used to relate the NMR data to the diffusion parameters in analogy to the case of the spherical top presented in Eqs. (19) and (22). Diffusion coefficients derived from the NMR frequency time-correlation function may then be used to determine the major and minor semiaxes of revolution of an ellipsoid, a and b , respectively, using¹⁸⁻²⁰

$$D_{\parallel} = \frac{3kT}{32\pi\eta} \frac{2a - b^2 G(a, b)}{(a^2 - b^2)b^2}, \quad (33a)$$

$$D_{\perp} = \frac{3kT}{32\pi\eta} \frac{(2a^2 - b^2)G(a, b) - 2a}{a^4 - b^4}, \quad (33b)$$

where

$$G(a, b) = \frac{2}{\sqrt{a^2 - b^2}} \ln \left(\frac{a + \sqrt{a^2 - b^2}}{b} \right) \quad (34a)$$

for $a > b$ (prolate ellipsoid), and

$$G(a, b) = \frac{2}{\sqrt{b^2 - a^2}} \arctan \left(\frac{\sqrt{b^2 - a^2}}{a} \right) \quad (34b)$$

for $a < b$ (oblate ellipsoid). Although the two diffusion coefficients in Eqs. (33a) and (33b) are indeterminate at $a = b$, they tend towards the value for the isotropic rotational diffusion coefficient given in Eq. (10) as $a \rightarrow b$.

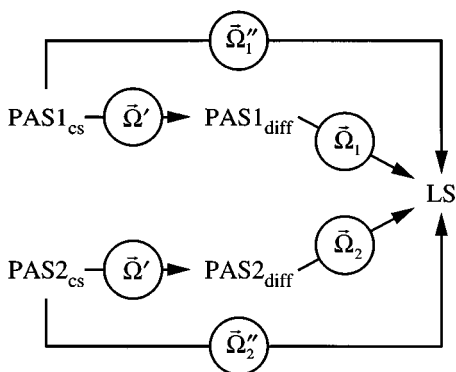


FIG. 4. Order of rotations relating the PAS of the CSA tensor, the PAS in which the diffusion tensor of the symmetric top is diagonal, and the LS. Note that $PAS1_{cs}$ and $PAS2_{cs}$ remain fixed with respect to the PAS of the diffusor.

F. Simulation of two-dimensional exchange spectra: Isotropic rotational diffusion

Up to this point we have focused on extracting time-correlation functions from the two-dimensional exchange spectrum with the assumption that the motional process is rotational diffusion. Even if the particle reorientation is not described by rotational diffusion, the frequency weighted integral of the exchange spectrum may still yield a monotonically decreasing function which may be fit with a sum of

decaying exponentials. Unlike the time-correlation function, two-dimensional exchange spectra can show features which are characteristic of anisotropic motions, discrete jumps, coherent rotation, etc.^{1-3,7} In order to gain more insight into the actual dynamics which we are observing, we need to develop a method of simulating two-dimensional exchange spectra based upon the rotational diffusion model. Simulations will allow us to determine if the process *looks* like rotational diffusion and to check for experimental artifacts.

The task of simulating two-dimensional exchange spectra using Eq. (6) appears very formidable. One must integrate over six separate angles over the interval $(0, 2\pi)$ for four of the angles and $(0, \pi)$ for the other two. Such a simulation would prove very difficult to solve in any reasonable amount of time. A simpler equation which takes into account redundant integrations has been derived previously by Wefing *et al.*^{2,3} In the simplification, Wefing approaches the problem from the point of view of a fixed chemical shift PAS where the LS appears to reorient from LS1 to LS2. The relative orientation of the two laboratory systems is $\mathbf{z}' = (\alpha', \beta')$, and the orientation of LS1 with respect to the PAS is $\mathbf{z}_1 = (\alpha_1, \beta_1)$. In the case of isotropic rotational diffusion and nonzero asymmetry parameter ($\eta \neq 0$), Eq. (6) reduces to

$$S(\omega_1, \omega_2; t_m) = \int_0^{\pi/2} d\beta' \sin(\beta') \Gamma^g(\beta', t_m) \int_0^{\pi/2} d\alpha_1 \\ \times \int_0^{\pi/2} d\beta_1 \sin(\beta_1) \delta[\omega(\alpha_1, \beta_1) - \omega_1] \\ \times \int_0^{2\pi} d\alpha' \delta[\omega(\alpha', \beta', \alpha_1, \beta_1) - \omega_2], \quad (35)$$

where

$$\Gamma^g(\beta', t_m) = \sum_{l=0}^{\infty} \frac{4l+1}{8\pi^2} \exp[-2l(2l+1)D^l t_m] \\ \times P_{2l}[\cos(\beta')], \quad (36)$$

$\omega(\alpha_1, \beta_1)$ is given in Eq. (1), and $\omega(\Delta\alpha, \Delta\beta, \alpha_1, \beta_1)$ may be determined using Eq. (29). Γ^g is referred to as either the jump or reorientation angle distribution.

As an example, Fig. 5 shows two-dimensional exchange spectra with nonzero asymmetry parameter for a number of correlation times with a fixed mixing time. The simulations were performed with steps of $\pi/64$ radians with each simulation requiring approximately 43 s of cpu time on a Silicon Graphics Indigo computer running a MIPS R4000 cpu. At zero mixing time, the spectrum should lie entirely along the diagonal from the bottom left hand corner to the top right hand corner.

We have chosen to perform the simulation in the frequency domain as opposed to the time domain to reduce the number of numerical operations. Each angle is independently sampled using equally spaced intervals which are chosen to produce acceptable gridding artifacts after the convolution of the spectrum with a two-dimensional Gaussian line broaden-

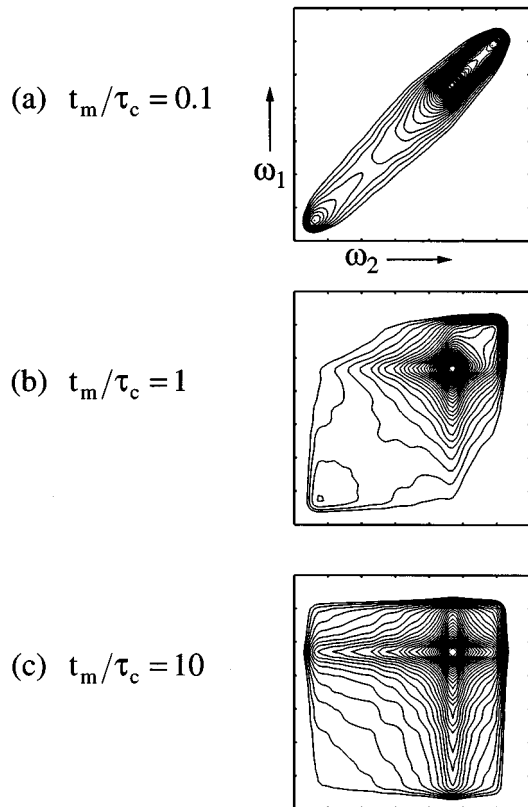


FIG. 5. Simulated ^{13}C two-dimensional exchange spectra with $\eta=0.45$. Some features present in the spectra are due to the finite sampling of orientations. Spectra are normalized to a maximum height of one.

ing function. The line broadening simulates the residual heteronuclear dipolar line broadening present from incomplete decoupling of the ^{13}C nuclei from the surrounding ^1H nuclei. CSA parameters are scaled in such a way that the computed angle dependent frequency corresponds to the appropriate matrix index of the spectrum preventing the need to rescale the NMR frequency at each point of the sampled grid of orientations. Instead, the resulting frequency is converted to an integer and the appropriate weighting is added to the spectrum elements indicated by the computed frequencies. Wefing has pointed out that simulation in the time domain is a better approximation to the real signal,² but the difference between the two methods is not important when one only wishes to use the simulation as a qualitative comparison to the experimental data. We have performed both time domain and frequency domain simulations and found no noticeable qualitative difference after the convolution of the spectrum with a Gaussian apodization function. In addition, NMR frequency time-correlation values derived from the simulated spectra using Eq. (22) agree with the correlation times used in the simulation. A detailed explanation of the simulation algorithm and associated source code written in C is available and may be requested from the first author.

Simulation of equivalent sites undergoing isotropic rotational diffusion with different correlation times involves almost no extra computation. It is sufficient to compute a reorientation angle distribution for each site independently and then add the distributions together weighted by the respective fractional population of each site. The resulting reorientation angle distribution may then be used in the simulation in the same way as the single correlation time reorientation angle distribution is used. As the calculation time of the reorientation angle distribution is much smaller than the total time required for the simulation, this method is more efficient than simulating the exchange spectrum separately for each correlation time and then adding the spectra. Examples of this sort of simulation will be presented later in this paper in association with the experimental results.

III. EXPERIMENTAL EXAMPLE: ISOTROPIC ROTATIONAL DIFFUSION OF LATEX SPHERES IN SUSPENSION

Latex microspheres are often used as prototypical spherical colloidal particles in DLS studies of rotational diffusion. Monodisperse latex microspheres are relatively easy to produce using emulsion polymerization reactions, have a density near that of water and, therefore, remain in suspension for long periods of time without the need for agitation of the sample. Furthermore, crystalline latex microspheres have been produced with an intrinsic optical anisotropy⁴ which is useful if one wishes to measure the rotational diffusion of spherical particles using DDLS.

The requirements for an acceptable colloidal suspension to be studied using two-dimensional exchange NMR differ somewhat from those in DDLS. As is the case for optical techniques, the particles should be monodisperse, relatively easy to synthesize and neutrally buoyant in the suspending

fluid. If the ^{13}C CSA interaction is to be used as the orientational probe, the particles should be relatively easy to enrich in ^{13}C at a site which is, preferably, not directly bonded to hydrogen; an absence of directly bonded protons considerably reduces the necessary decoupling power during the evolution and detection periods. Furthermore, the functional group containing the ^{13}C probe should not undergo significant reorientation within the particle during the mixing time. Since spin-lattice relaxation times of ^{13}C nuclei in solid polymers are on the order of 1 s and the inhomogeneous linewidths are on the order of 100 ppm, measurable correlation times range from 5 ms to 1 s. At room temperature with water as the suspending fluid, these correlation times require the particles have a radius between 170–1000 nm.

In order to avoid excessive background signal, the suspending solvent should be free of ^{13}C nuclei, so common organic solvents are not appropriate. In light of its ease of use and availability, water is used as the suspending fluid in this study. Alternative solvents such as ^{13}C depleted organic solvents and silanes may be preferable for specialized applications.

The results reported here are for a colloidal suspension of PMMA microspheres enriched to approximately 20% ^{13}C at the carbonyl site with a target radius of 300 nm. The method of synthesis for small batches of the particles is presented in detail below.

A. Preparation of methyl ^{13}C -(carbonyl)-methacrylate

Methacrylic acid enriched to 100% ^{13}C at the carboxylic acid group is synthesized by the low temperature carboxylation of isopropenyl magnesium bromide with barium carbonate- ^{13}C .²¹ The acid is then isolated as the sodium salt and dried at 110 °C under high vacuum. Esterification of the salt proceeds with trimethylphosphate on a vacuum manifold system in the presence of hydroquinone to inhibit polymerization. The resulting methyl ^{13}C -(carbonyl)-methacrylate is isolated by low temperature distillation. The final yield with respect to the barium carbonate- ^{13}C reactant is between 75% and 80%. Both the yield and sample purity obtained by this synthesis are higher than a previously reported reaction sequence via acetone cyanohydrine (from acetone and potassium cyanide- ^{13}C).²²

B. Preparation of ^{13}C -(carbonyl)-poly(methyl methacrylate) microspheres

The preparation of the enriched ^{13}C -(carbonyl)-poly(methyl methacrylate) (PMMA) latex microspheres is complicated by the fact that only a small quantity may be produced due to the high cost of the enriched MMA reactant. From previous experience, we have found that it is difficult to synthesize very small quantities of high quality microspheres in a single-step emulsion polymerization reaction. A more reliable method in this case is to perform a two-step semicontinuous emulsion polymerization where the enriched MMA is polymerized onto the surface of smaller, unenriched, monodisperse seed particles; the seed particles are

produced in a large quantity to ensure their high quality. The following details the synthesis of approximately 300 nm radius enriched PMMA microspheres with a 125 nm unenriched core.

In the first step, seed particles of unlabeled MMA with a radius of 125 nm are synthesized in a 1 L reaction vessel in the presence of nitrogen to avoid the reaction of oxygen with the monomer. For the synthesis 200 mL of H₂O, 25.0 mL of a 0.5% solution of polyethyl ether (AD33[®], Atochem, France) to act as an emulsifier, 20 mL of a 1.57% solution of (NH₄)₂S₂O₈ to act as an initiator, and 15.0 g unenriched MMA are initially placed in the reactor. After a nucleation time of 2 h at 20 °C, a pre-emulsion composed of 177 g MMA, 50 mL of a 1.0% solution of AD33[®], and 200 mL of H₂O is pumped into the main reactor at a rate of 3.6 mL/min. Simultaneously, 25 mL of a 1.57% solution of the initiator (NH₄)₂S₂O₈ is added at a rate of 0.21 mL/min. The reaction temperature is stabilized at 72 °C with a stirring speed of 250 rpm. After the addition is complete, the temperature is raised to 85 °C for 5 h in order to obtain high conversion and to dissociate the remainder of the initiator. The final solids content is 27.3% by weight.

In the second step, the labeled MMA polymerized onto the surface of the 125 nm latex seed particles in a 50 mL reactor. The synthesis of 300 nm particles is very difficult because the MMA has a tendency to spontaneously nucleate during the addition of the monomer. To avoid the formation of new particles in this step of the synthesis, the addition rate is slowed down, and the concentration of emulsifier is reduced to suppress unwanted nucleation in micelles formed by the emulsifier. It should be noted that a certain amount of emulsifier is necessary for the stabilization of the emulsion, so the emulsifier cannot be completely removed.

For the reaction, 462 mg of the seed latex and 13.4 g of H₂O are added to the main reactor. A pre-emulsion composed of 917 mg of the enriched MMA, 983 mg of a 1% solution of AD33[®], 1.68 g of a 1.57% solution of (NH₄)₂S₂O₈, and 1.54 g of H₂O is added over a period of 4 h with a 5 mL syringe. The temperature in the 50 mL reactor is stabilized at 72 °C during the addition and is then raised to 85 °C for 26 h after the addition to ensure completion of the polymerization. The final solids content of the colloidal suspension is 10% by weight.

C. Size characterization of the latex microspheres

The size of the latex microspheres was investigated by both dynamic light scattering techniques and by scanning electron microscopy (SEM).

DLS, being the customary method for size characterization, was used initially. Measurements performed on an Autosizer 4700 (Malvern) indicated a particle radius of approximately 313 nm with a polydispersity of 10%. There was no indication of particles with a substantially different size. Rotational diffusion measurements made using two-dimensional exchange NMR did not agree with this result as will be shown below.

To resolve the discrepancy, SEM measurements were

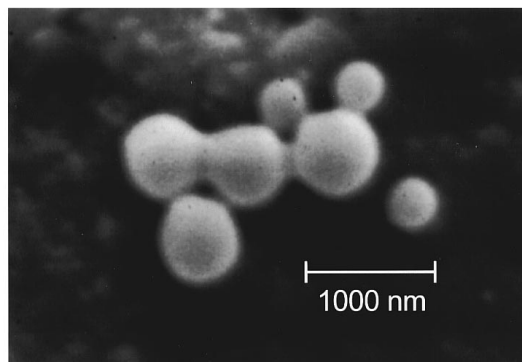


FIG. 6. Scanning electron micrograph of the PMMA microspheres coated with approximately 25 nm of gold. Measurements from this image indicate particle radii of 320 ± 40 nm and 180 ± 40 nm. These values take into account the 25 nm layer of gold on the surface of the particles. Uncertainty arises from the 80 nm wide indistinct outline of the particles in the image. Radius measurements were made from the central point of the indistinct outline using the image analysis program NIH Image 1.52.

made using a Microscope Stereoscan (Cambridge Instruments) with an acceleration voltage of 8 kV. One droplet of the latex was diluted with 2 mL of water, applied to an aluminum support, freeze dried, and gold coated using an Auto Sputter Coater (Bio-Rad, Polaron Division). Particle sizes determined from the SEM micrograph in Fig. 6 indicate the presence of particles with two distinct radii, 320 ± 40 nm and 180 ± 40 nm. The uncertainty reflects blurring of the microsphere edges in the picture. It appears that a second nucleation at a relatively early stage in the reaction has taken place. This would imply that the larger particles contain a 125 nm radius unenriched core, whereas the smaller particles are composed entirely of enriched PMMA.

D. Two-dimensional exchange NMR experiment

Figure 7 shows the pulse sequence used in the two-dimensional exchange experiment. The initial ¹³C magnetization is created by cross polarization from ¹H nuclei, and evolves for a time t_1 . During the evolution period, a decoupling field is applied to quench the dipolar interaction between the ¹³C and ¹H nuclei. After the evolution period, a $\pi/2$ pulse stores one component of the ¹³C magnetization along the direction of the static field. Neglecting spin-lattice relaxation, the stored magnetization does not evolve during the mixing period. The second ¹³C $\pi/2$ pulse returns the stored magnetization to the plane perpendicular to the static

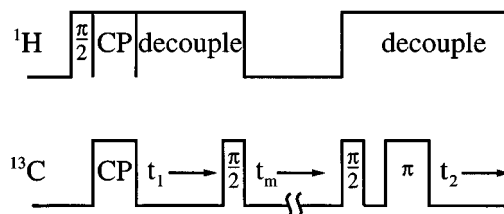


FIG. 7. NMR pulse sequence for the two-dimensional NMR exchange experiment using a $9 \mu\text{s}$ ¹H excitation pulse, 1.5 ms cross polarization contact time, and 2.1 ms acquisition time with a spectral width of ± 15 kHz.

field for detection accompanied by decoupling. In order to ensure that the signal at $t_2=0$ is acquired, a π pulse is performed to create a spin echo. The addition of the spin echo makes it unnecessary to apply a first order phase correction along t_2 , so we are only required to apply a zero order phase correction to the resulting two-dimensional exchange spectrum. The experiment is repeated with increasing values of t_1 until a sufficient number of t_1 points have been acquired. The method of States²³ is used to obtain a pure-phase absorption spectrum.

The $t_1=0$ slice in each two-dimensional exchange experiment was analyzed in order to determine the CSA parameters of the carbonyl carbon in the PMMA sample. These parameters are used for the determination of the NMR frequency time-correlation function, Eq. (22). Calculations yield a value of 90 ppm for δ and 0.45 for η . Values for the isotropic shift vary slightly between experiments and are calculated separately for each exchange spectrum. All experiments were performed on a 300 MHz home-built homodyne spectrometer²⁴ controlled by a Tecmag pulse programmer and a Macintosh IIfx computer. The achieved ^{13}C and ^1H radio-frequency nutation rates of 27 kHz provided acceptable decoupling of the ^{13}C - ^1H dipolar interaction and pulse times short enough to make it unnecessary to perform a first order phase correction along the t_1 encode dimension.

Since experiments for separate mixing times are run for approximately 12 h, significant settling of the latex microspheres is expected. To eliminate particle sedimentation, the sample is placed in a KelF tube with a pulley/cap, supported on KelF/Teflon bearings, which is slowly rotated within the rf coil by a belt drive connected to an electric motor external to the magnet. Rotation at ~ 0.05 Hz prevents sedimentation but does not affect the exchange spectra for the short mixing times used.

Two-dimensional exchange NMR experiments were also run with dry PMMA particles to determine the extent of carbonyl reorientation within the solid. No appreciable motion (i.e., exchange) was observed for mixing times similar to those used in the study of the colloidal suspension.

E. Results

Two-dimensional NMR exchange experiments were performed for a number of mixing times chosen to adequately sample the decay of the NMR frequency time-correlation function. Figure 8, a plot of the natural logarithm of the time-correlation function vs the mixing time, shows the presence of at least two exponentially decaying components corresponding to distinct correlation times. We will consider two possible explanations for the presence of multiple correlation times. The first and more likely model in light of the means by which the sample is prepared assumes the presence of spherical particles with two distinct radii, and the second model assumes that the sample is composed of ellipsoidal particles. Although the SEM evidence, Fig. 6, clearly supports the former model, both results will be presented, since analysis of the NMR exchange data was begun before the SEM measurements were performed.

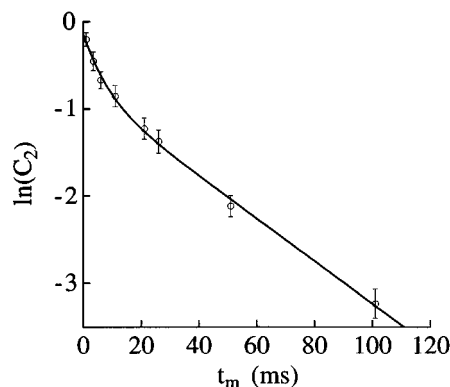


FIG. 8. Plot of the natural logarithm of the NMR frequency time-correlation function vs mixing time derived from the results of a series of two-dimensional NMR exchange experiments. The data are fit to the four parameter biexponential function given in Eq. (37). Vertical error bars represent the possible error due to setting the integration window inside of and outside of the correct integration window. Due to the finite time involved in signal acquisition and evolution during t_1 , an error of ± 1 ms in time exists for each point.

A biexponential function,

$$f(A, p_1, \tau_1, \tau_2; t_m) = \ln \left\{ A \left[p_1 \exp \left(-\frac{t_m}{\tau_1} \right) + (1 - p_1) \exp \left(-\frac{t_m}{\tau_2} \right) \right] \right\}, \quad (37)$$

shown as a solid line in Fig. 8 fits the data well. The adjustable parameters used in the fitting process are as follows: A takes into account effects of line broadening due to ^{13}C - ^1H dipolar coupling, p_1 is the fraction of signal contributed by particles with a rotational diffusion correlation time τ_1 , and τ_2 is the correlation time for the other sized particles. The following values yield the best fit,

$$\begin{aligned} \tau_1 &= 6.4 \pm 1.5 \text{ ms}, \\ \tau_2 &= 41.8 \pm 2 \text{ ms}, \\ p_1 &= 0.49 \pm 0.015, \\ A &= 0.85 \pm 0.04. \end{aligned} \quad (38)$$

The reported errors reflect the uncertainty in determining the proper limits of integration for the extraction of the time-correlation function from the exchange spectrum.

Assuming a temperature of 300 K and a viscosity of 1.0×10^{-2} Poise, the two correlation times correspond to the radii 180 ± 13 nm and 338 ± 5 nm. These values agree very well with those determined by scanning electron microscopy, Fig. 6, and the presence of two particle sizes is attributed to spontaneous nucleation during the second step of the polymerization reaction. The relative number of small to large particles is calculated to be 6:1 assuming the smaller particles are composed entirely of the 20% enriched PMMA and the larger particles contain a core of unenriched PMMA.

Due to the finite duration of the acquisition and encode times (~ 2.1 ms), each point in Fig. 8 has an uncertainty of

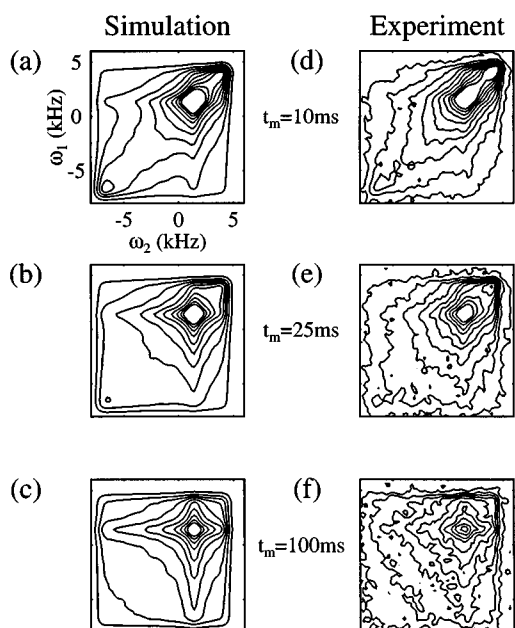


FIG. 9. Experimentally obtained two-dimensional exchange spectra and their corresponding simulations. The simulations assume two correlation times, 6.4 ms and 41.8 ms, with equal weighting. All spectra are normalized with respect to the integral over the entire spectrum, and are plotted from -8 kHz to 6 kHz along both frequency axes. Contour levels represent steps of 10% with respect to the maximum amplitude in (f).

± 1 ms. This uncertainty is substantial compared to the shorter correlation time, so it is surprising that the particle size determined from this correlation time agrees so well with the SEM data. On the other hand, the uncertainty is substantially smaller than the longer correlation time, so we would expect the NMR data to provide a reasonably accurate estimate of the larger particle size.

A fit (not shown) to the data in Fig. 8 employing the symmetric top model of Sec. II E yields the values $D_{\parallel} \cong 30$ Hz and $D_{\perp} \cong 2.6$ Hz. Assuming the particles to be prolate ellipsoids, Eqs. (33a), (33b), and (34a) indicate a major semi-axis of 740 nm and a minor semi-axis of 104 nm. These values are not consistent with either the expected shape of particles produced by the emulsion polymerization technique, or the apparent particle sizes determined by SEM, Fig. 6. The two diffusion coefficients are inconsistent with the model of an oblate ellipsoid, Eq. (34b).

Figure 9 shows a comparison of some of the experimentally obtained exchange spectra with simulations using the two measured correlation times in Eq. (38). The simulations are line broadened in the time domain using a 2 kHz Gaussian apodization function, and the experimental data has been line broadened by 1 kHz to reduce the effect of noise in the plot. All of the datasets have been normalized with respect to the volume under the spectrum, so a comparison of the contour levels between experiment and simulation is justified. Qualitatively, the simulations agree very well with the experimental data.

IV. CONCLUSIONS AND OUTLOOK

The results presented here show that two-dimensional exchange NMR provides a means of investigating the reorientational dynamics of particles for correlation times ranging from milliseconds to seconds. In fact, while routine DLS measurements indicated a single particle size in the sample prepared for these experiments, the NMR exchange experiments correctly indicated the presence of two distinct particle sizes as evidenced by the SEM results.

For the colloidal suspension used in this study, it was necessary to signal average for approximately 12 h for each two-dimensional exchange spectrum in order to obtain spectra with a sufficiently high signal to noise ratio (S/N) to clearly show all spectral features. However, a considerably lower S/N is tolerable when the only purpose of the experiment is to obtain values of the time-correlation function. The length of the experiment may then be reduced by as much as a factor of 10, allowing the determination of a single point of the time-correlation function in approximately 1 h. For a more concentrated sample, the length of the experiment may again be reduced. An increase in the particle concentration by a factor of 4 allows the acquisition of a two-dimensional exchange spectrum with S/N comparable to the spectra presented in this work in 45 min, and a single point in the time-correlation function can be acquired in as little as 5 min.

The improved signal to noise with increased concentration makes two-dimensional exchange NMR well suited for studying reorientational processes in sediments, slurries, pastes, or any other system with high particle concentrations. The technique also promises to be useful in studying particle dynamics in turbulent, non-Newtonian, and solid particle flow. Of course, for the above examples the motion is not necessarily rotational diffusion, so the interpretation of the exchange spectra will require consideration of other appropriate models for the reorientational processes. Given sufficient signal, NMR exchange experiments may be combined with imaging techniques to correlate reorientational dynamics with spatial maps or translational motion. Stimulated echo exchange experiments²⁵ which do not require the acquisition of the entire two-dimensional time domain data set may be especially useful in this case.

The orientational probe used in this work, the CSA of the ^{13}C nucleus, is suitable for measuring reorientational processes with correlation times ranging from milliseconds to one or two seconds. Using deuterium as a probe allows the investigation of time scales approximately one order of magnitude shorter.^{3,7} For shorter times, two-dimensional exchange pulsed EPR may prove useful.

ACKNOWLEDGMENTS

We would like to thank Dr. Matthias Ernst for checking the results relating to the time-correlation functions of symmetric tops. This work was supported by the Director, Office of Basic Energy Sciences, Materials Sciences Division, and the Director, Office of Health and Environmental Research, Health Effects Research Division, of the U.S. Department of

Energy under Contract No. DE-AC03-76SF00098. This work was presented in part at the 35th Experimental Nuclear Magnetic Resonance Conference, Asilomar, CA, March 1994; Abstract #WP180.

- ¹K. Schmidt-Rohr and H. W. Spiess, *Multidimensional Solid-State NMR and Polymers* (Academic, San Diego, 1994).
- ²S. Wefing and H. W. Spiess, *J. Chem. Phys.* **89**, 1219 (1988).
- ³S. Wefing, S. Kaufmann, and H. W. Spiess, *J. Chem. Phys.* **89**, 1234 (1988).
- ⁴R. Piazza and V. Degiorgio, *Phys. Rev. B* **42**, 4885 (1990).
- ⁵R. Piazza and V. Degiorgio, *Physica A* **182**, 576 (1992).
- ⁶*Dynamic Light Scattering: Applications of Photon Correlation Spectroscopy*, edited by R. Pecora (Plenum, New York, 1985).
- ⁷C. Schmidt, B. Blümich, and H. W. Spiess, *J. Magn. Reson.* **79**, 262 (1988).
- ⁸U. Haeberlen, *High Resolution NMR in Solids: Selective Averaging* (Academic, New York, 1976).
- ⁹M. E. Rose, *Elementary Theory of Angular Momentum*, 1st ed. (Wiley, New York, 1957).
- ¹⁰J. Jeener, B. H. Meier, P. Bachmann, and R. R. Ernst, *J. Chem. Phys.* **71**, 4526 (1979).
- ¹¹D. L. Favro, *Phys. Rev.* **119**, 53 (1960).
- ¹²E. N. Ivanov, *Sov. Phys. JETP* **18**, 1041 (1963).
- ¹³P. J. W. Debye, *Polar Molecules* (The Chemical Catalog Company, New York, 1929).
- ¹⁴R. B. Jones, *Physica A* **150**, 339 (1988).
- ¹⁵B. J. Berne and R. Pecora, *Dynamic Light Scattering* (Wiley, New York, 1976).
- ¹⁶R. B. Jones, *Physica A* **157**, 752 (1989).
- ¹⁷K. Schmidt-Rohr and H. W. Spiess, *Phys. Rev. Lett.* **66**, 3020 (1991).
- ¹⁸The equation given by Berne and Pecora [p. 143, Eq. (7.7.1)] for the rotational diffusion coefficient characterizing diffusion about the axis of symmetry appears to be incorrect.
- ¹⁹F. Perrin, *J. de Phys. et Rad.* **5**, 497 (1934).
- ²⁰F. Perrin, *J. de Phys. et Rad.* **7**, 1 (1936).
- ²¹M. Hasegawa, S. Ohyabu, T. Ueda, and M. Yamaguchi, *J. Labelled. Compd. Radiopharm.* **18**, 643 (1981).
- ²²K. Schmidt-Rohr, A. S. Kulik, H. W. Beckham, A. Ohlemacher, U. Pawelzik, C. Boeffel, and H. W. Spiess, *Macromolecules* **27**, 4733 (1994).
- ²³D. J. States, R. A. Haberkorn, and D. J. Ruben, *J. Magn. Reson.* **48**, 286 (1982).
- ²⁴Y. K. Lee, doctoral thesis, University of California at Berkeley, 1994.
- ²⁵F. Fujara, S. Wefing, and H. W. Spiess, *J. Chem. Phys.* **84**, 4579 (1986).